AUBE '01

12TH INTERNATIONAL CONFERENCE ON AUTOMATIC FIRE DETECTION

March 25 - 28, 2001
National Institute Of Standards and Technology
Gaithersburg, Maryland U.S.A.

PROCEEDINGS

Editors: Kellie Beall, William Grosshandler and Heinz Luck

NIST CENTENNIAL 1901-2001

EUSAS

NIST
National Institute of Standards and Technology
Technology Administration, U.S. Department of Commerce

Thomas Cleary and Michelle Donnelly
Building and Fire Research Laboratory, National Institute of Standards and Technology
Gaithersburg, MD, 20899 U.S.A.

Aircraft Cargo Compartment Fire and Nuisance Source Tests in the FE/DE

1. Introduction

Commercial transport aircraft cargo compartments require both fire detection and suppression capabilities in order to meet regulatory requirements. Historically, while there have been few fires reported in cargo compartments, false alarms are a much more frequent event. A recent study places the false alarm to smoke detection ratio at 200:1 over the last five years [1]. A significant fraction of false alarms is thought to be due to nuisance sources such as condensed water vapor, and other aerosol sources [2]. The Federal Aviation Administration requires that detectors meet standards in **SAE** AS 8036 (wherein UL smoke box testing is referenced as appropriate to check alarm sensitivity) which specifies that the alarm must fall between 60 %/ft to 96 %/ft light transmission (extinction coefficients between 3.0 m^{-1} to 0.13 m^{-1}) [3]. Each new cargo compartment design must pass a system test on the ground and in-flight using "smoke" which may be produced from aerosol generators, tobacco smoldering or other non-fire sources. An alarm must be recorded within 60 s of the start of the aerosol source. The FAA is developing standard flaming fire and smoldering fire sources that will be more repeatable than the range of aerosol sources currently in use, and that will allow other types of detectors besides smoke detectors to be qualified. In a recent survey of fire detection technologies, gas and thermal sensing were identified as plausible additions to particulate sensing in cargo compartments to improve detection [4]. Here, fire and nuisance scenarios were emulated in the fire emulator/detector evaluator (FE/DE), and gas, thermal and particulate sensor signals were gathered to determine potential sensor combinations that would overcome various nuisance alarm events in cargo compartments. The selection of the flaming, smoldering, and nuisance alarm scenarios was guided by a desire to cover a range of potential fire and nuisance alarm scenarios that would each progress to a point were current aircraft detectors would alarm; there was no basis for these scenarios from statistical analysis of fire data, nor service difficulty reports addressing false alarms.

2. Fire and Nuisance Alarm Scenarios

Two separate flaming, smoldering, and nuisance scenarios tailored for aircraft cargo compartments were emulated in the FEDE and are described here. Additional scenarios are described in a MST report [5]. The FE/DE is a 0.3 m high by **0.6** m wide cross-section flow tunnel designed to reproduce the time-varying speed, temperature and concentration (gas and particulate) expected at detector locations in the early stages of the fire (Figure 1). The FEDE employs a variable speed blower and resistance heaters to control velocity and temperature (ambient and higher) over ranges of 0.02 m/s to greater than 1 m/s and **20 °C** to **80** °C, respectively.

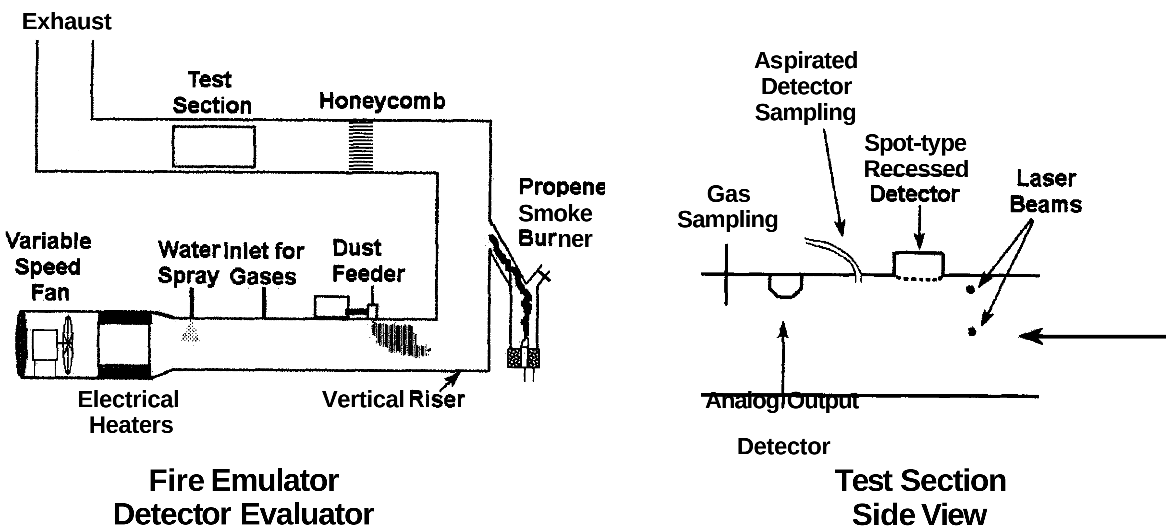

Figure 1. Schematic of fire emulator/detector evaluator.

The fire sources chosen for this study cover **a** wide range of fire phenomena. They consist of the following: (1) a flaming fire indicative of a plastic or liquid hydrocarbon pool fire, **(2)** a "low-smoke" flaming fire that consists of ethanol-soaked cotton-polyester blend fabric, **(3)** a smoldering cotton wick fire, and **(4)** a pyrolyzing mixed plastics plaque obtained from the **FAA** Technical Center. Two nuisance sources chosen to represent potential source of false alarms due to environmental conditions in aircraft cargo compartments were emulated. They consist of the following: (1) dust exposure, and **(2) an** oil mist aerosol.

Measurements of laser light extinction, temperature, gas concentration and analog output detectors at the test section were made to characterize the fire and nuisance sources. These measurements are indicative of sensor outputs that could be part of a multi-sensor detector. Light extinction measurements are made across the tunnel duct at the test section. The light transmission path across the 0.60 m wide duct is extended to 1.50 m by reflecting the laser beam off two mirrors placed inside the duct. The beam is split outside the tunnel resulting in two parallel beams, one at 4 cm and one at 15 cm (mid-height) below the top of the duct. Photodetectors are positioned on the opposite side of the duct to record the transmitted light intensity. In smoke-free air, the photodetector output fluctuates randomly +/- 0.1 % about the mean intensity. The extinction coefficient, k (m^{-1}) is obtained from the following equation:

$$\frac{I}{Io} = \exp^{-kL} \qquad [1]$$

I_0 is the smoke-free light intensity, while I is the intensity when smoke is present, and L is the path length (m). Process gas analyzers recorded CO, CO_2, and water content in the air from samples drawn from the test section. The instrument ranges are **0** to **5** $\times 10^{-4}$ volume fraction CO and 0 to 0.04 volume fraction CO_2. The uncertainty of the measurements are stated as **2.5** $\mathbf{\times 10^{-6}}$ volume fraction CO and **2** $\mathbf{\times 10^{-5}}$ volume fraction $\mathbf{CO_2}$. The water analyzer range is **0** to 0.05 volume fraction with an expanded uncertainty of 10 % of the measurement. The response time for these analyzers **(90%** of ultimate response to a step change) is **15** s. An electrochemical CO sensor was placed in the tunnel and its output recorded, then converted to CO volume fraction. Air temperature was recorded by a type-K thermocouple constructed from **0.08** mm bare wire located 5 cm from the ceiling of the duct, and approximately 15 cm downstream from the laser beam. An analog output photoelectric, ionization, and thermal detector was located on the ceiling of the test section **30** cm downstream from the laser beam The output of this detector was previously "calibrated" against propene soot, dust and nebulized oil aerosol [6]. Two different aircraft smoke detectors were installed to indicate the smoke or nuisance source conditions that would cause existing detectors to alarm. The alarm conditions are suggestive of existing performance, however, these tests should not be considered detector performance tests. One detector **{D1}** was a spot-type photoelectric unit designed to be mounted on the ceiling of the cargo compartment. It has a low profile housing and is covered by a large-opening protective metal grate. It was installed at the ceiling location in the FEDE test section, mounted **as** it would be in a cargo compartment. The alarm point for this detector was set at an extinction coefficient of approximately **0.13** m^{-1} **(4 %/ft,** the most sensitive allowed by ***SAE*** **AS8036).** The other detector **{D2}** was a draw-through type detector that is designed to sample cargo compartment air through tubing with openings at the ceiling. The alarm point for this detector was set at an extinction coefficient of approximately 0.31 m^{-1} **(9** %/ft). This detector was installed outside the test section with a **15** cm long **6** mm I.D. plastic tube extending **2.5** cm below the duct ceiling as the sample point. The flow through the detector was set at approximately **4 L/min.**

3. Experimental Results

Test fire **1,** the flaming fire, emulates conditions developed as the result of a burgeoning hydrocarbon pool or burning plastics fire. The FEDE reproduced the flow conditions by control of the fan speed to achieve the expected ceiling jet velocity. The heater set point was controlled to provide the increasing temperature at the detector location. Smoke was provided from the propene smoke generator attached to the FEDE. The smoke generator **is** an annular co-flowing, air/propene diffusion burner contained in a steel duct with damper-controlled bypass and tunnel connections. The fan speed was set at **10 Hz** which yielded a mean core flow of **0.25 m/s** at the test section. The damper was opened at time = 0 to let smoke flow into the duct. Figures **2-4** show representative values of smoke extinction, combustion gases and air temperature for this scenario. The alarm time for the spot-type aircraft detector is marked on the extinction graph; the draw-through detector did not record an alarm. In Figure **2,** the extinction coefficient began to rise at **30 s,** (this delay represents the transport of the smoke from the smoke generator to the test section). At about **40 s,** both the photoelectric and ionization analog signals began to rise. The photoelectric signal reached its maximum output at **60 s** while the ionization signal continued to climb until leveling off at **120 s.** The ionization signal lagged the extinction value due to the smoke entry lag of the detector. Figure **3** shows CO, CO_2, and water volume fractions with background values subtracted.

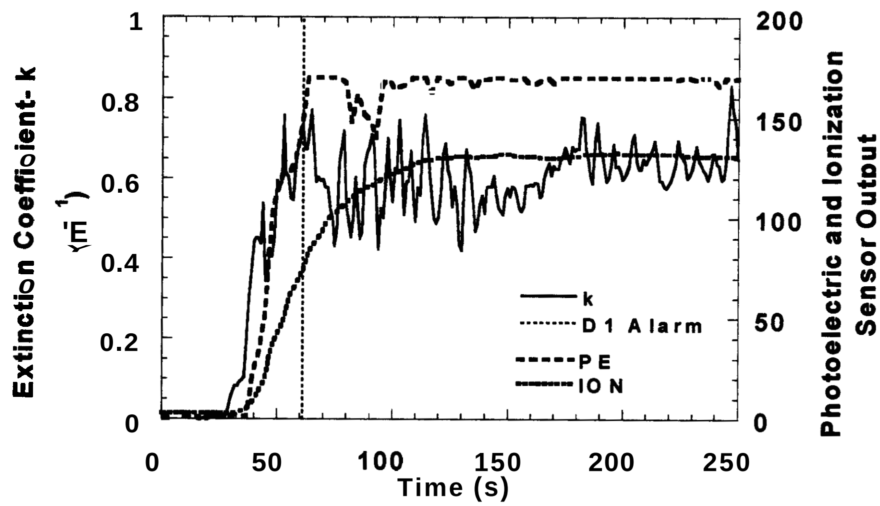

Figure 2. Smoke level for test fire 1: flaming fire.

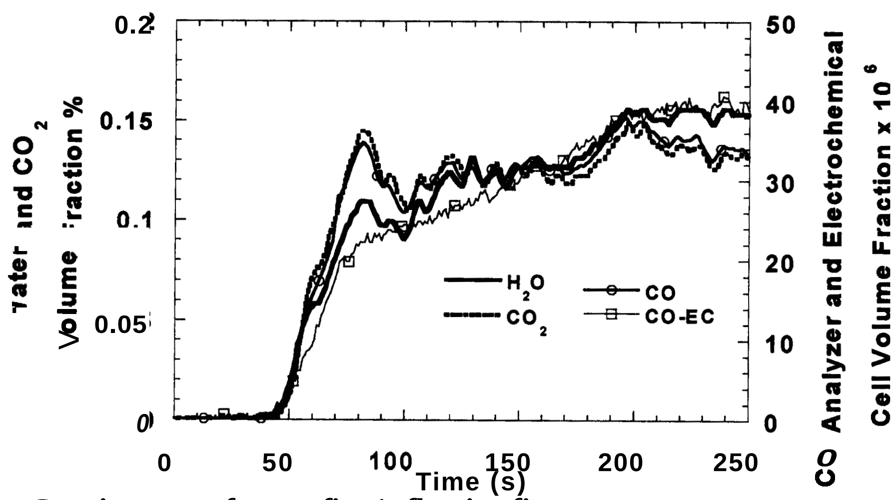

Figure 3. Gas **signatures for test fire** 1, **flaming fire.**

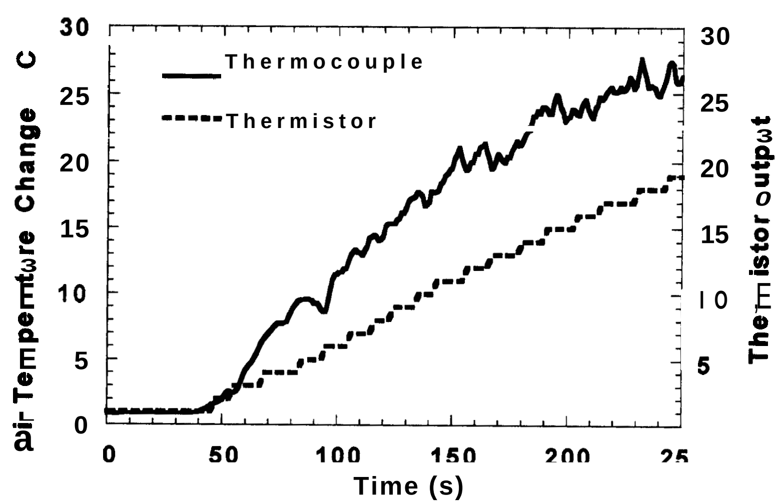

Figure 4. Temperature rise for test fire 1, **flaming fire.**

All gas concentrations began to rise at 45 **s** (time to transport gases to analyzers ≈ 15 **s).** The delayed response of the electrochemical cell is most likely due to diffusional transport delay of **CO** into the cell itself. The **C02** and water volume fractions are nearly identical which would be expected from nearly complete combustion of propene. The CO/CO_2 volume ratio is about 0.025, which is reasonable for the over-ventilated diffusion flame in the smoke generator. The temperature rate of rise averaged 0.13 **°C/s** from **40 s** to 250 **s** (Figure 4). The thermistor output lagged the fast-response thermocouple. This is a constant occurrence due to the relatively sluggish response characteristics of the thermistor compared to the fast-response thermocouple.

Test fire **2,** the low-smoke flaming fire, was designed to emulate conditions from a cargo compartment fire that begins by ignition of alcohol-soaked baggage where the initial effluent is very low smoke until the alcohol burns out and the fabric starts to burns. The result is a temperature rise and gas signature that precedes the measurable smoke at the test section. The fuel consisted of six **7 cm** diameter cotton/polyester (50/50 blend by weight) fabric circles stacked and held together with **3** staples, and wetted with ***5*** mL of ethanol. The wetted fabric was placed over a 10 **cm** glass dish and supported by two crisscrossed nichrome wires, then placed at the bottom of the vertical riser section of the FE/DE prior to ignition. The fan speed was set to 10 Hz (mean flow velocity of 0.25 m/s), then the alcohol was ignited at time = 0. At first, only the alcohol burned as it was wicked through the fabric or burned from excess in the dish below. During this phase, no appreciable smoke was produced. As the alcohol burned out, the fabric circles caught fire and burned with considerable smoke production, then burned out. Figures **5-7** show representative smoke, combustion gas production and temperature rise from this scenario. In Figure 5, the ionization signal started to rise at 20 **s** while the extinction and photoelectric signal started to rise at **60** s. The initial combustion produced an aerosol that was not scattering much light, but was being sensed by the ionization detector. As the fabric circles caught fire, the extinction coefficient and photoelectric signals began to rise. The extinction coefficient decayed much faster than the photoelectric or ionization signal due to hold-up of the heated smoke in the detector sensing volume. Figure **6** shows CO, CO_2 ,and water volume fraction with background values subtracted. At **25** s water and **C02** started to rise; initially, water was higher than the CO_2 which **is** expected

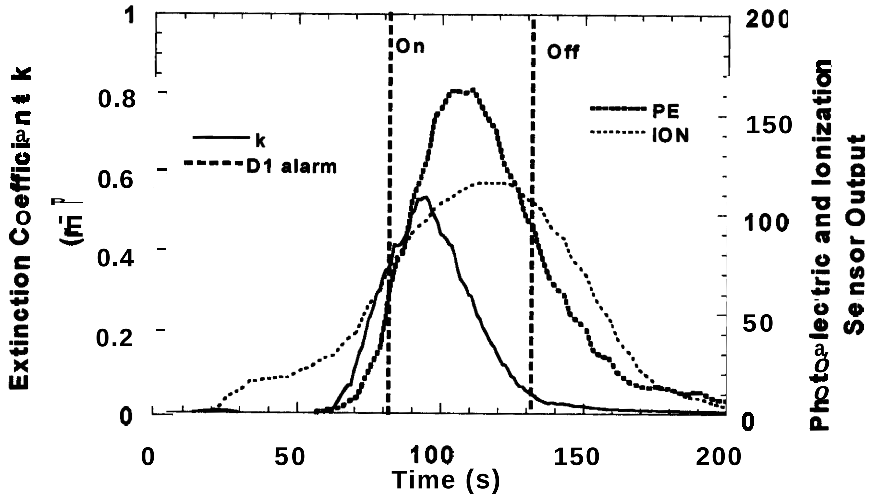

Figure 5. Smoke level for test fire 2, alcohol-soaked fabric fire.

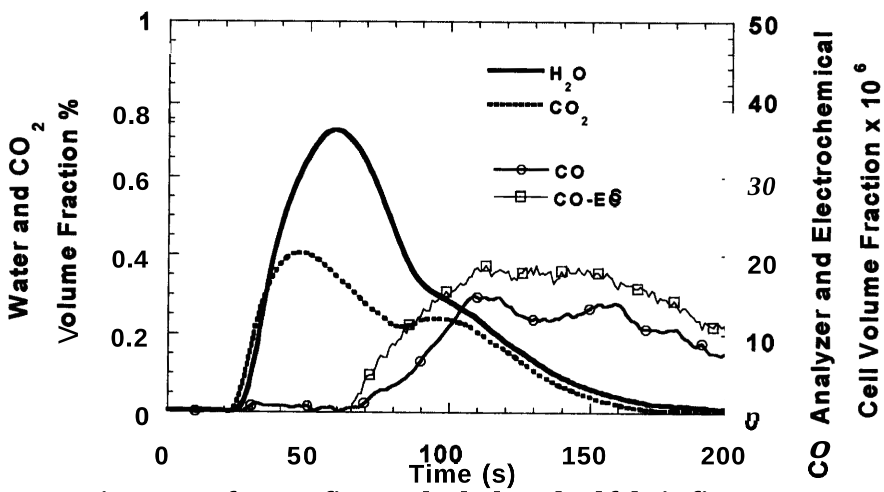

Figure 6. Gas signatures for test fire 2, alcohol-soaked fabric fire.

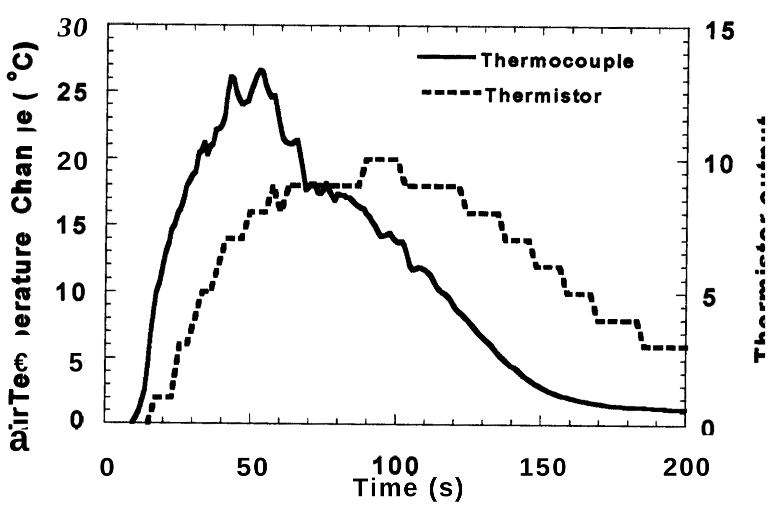

Figure 7. Temperature rise for test fire 2, alcohol-soaked fabric fire.

as the ethanol was burning. The CO concentration began to rise as the fabric started to burn and remained elevated even as the extinction decreased to near zero. The output of the electrochemical cell deviated from the CO analyzer and was most likely due to temperature and humidity effects of the cell output. Air temperature rose at a rate of nearly 1 °C/s, peaking at 27 °C above ambient (≈20 °C) 30 s after the initial rise (Figure 7).

Test fire 3, the smoldering cotton fire source, is a variant of a standard detector sensitivity test fire EN 54 part 9 test fire 3. A staged-wick-ignition test fixture developed for use in the FE/DE holds 32 cotton wicks 6 mm in diameter (typically 15 cm long) in a vertical orientation around a circular frame. Unique to the test fixture developed here is that each wick pair is spaced so that it is 5 cm away from adjacent pairs and the bottom of each wick passes through a wound nichrome ignition wire. Opposing pairs are wired in series producing a maximum of 8 independently ignited sets of 4 wicks. For the tests here, the objective was to produce a steadily increasing smoke concentration at the test section for 120 s. This was accomplished by igniting 8 sets of 4 wicks with a 12 s delay between each set. The fan was set to 10 Hi, yielding a mean velocity of 0.25 m/s at the test section, and the ignition sequence was started at time = 0. Figures 8 and 9 show representative smoke and combustion gas production for this source. In Figure 8, the extinction started to rise at 50 s followed by the ionization signal at 60 s and the photoelectric signal at 70 s. The photoelectric signal reached its maximum output at 115 s and both of the aircraft detectors alarmed between 130 s and 135 s. The extinction coefficient peaked at 140 s. In Figure 9, the gas concentrations began to rise between 60 s and 70 s, and peaked at about 170 s. The CO/CO_2 volume ratio is about 1:2.6, similar to the 1:3 ratio obtained in room tests with the same cotton smolder source [7]. The CO_2/water volume ratio is approximately 1:3. Air temperature rise peaked at 3.5 °C which is not uncharacteristic for low-energy-output smolder plumes

Test fire 4, pyrolyzing mixed plastics, uses the same smolder source being developed at the FAA Technical Center. It consisted of a 10 cm by 10 cm by 0.5 cm plaque of compressed plastic pellets, 2 mm to 5 mm in size with a nichrome wire embedded in it. The pellets were a mix of various plastics. The plaque was placed at the bottom of the

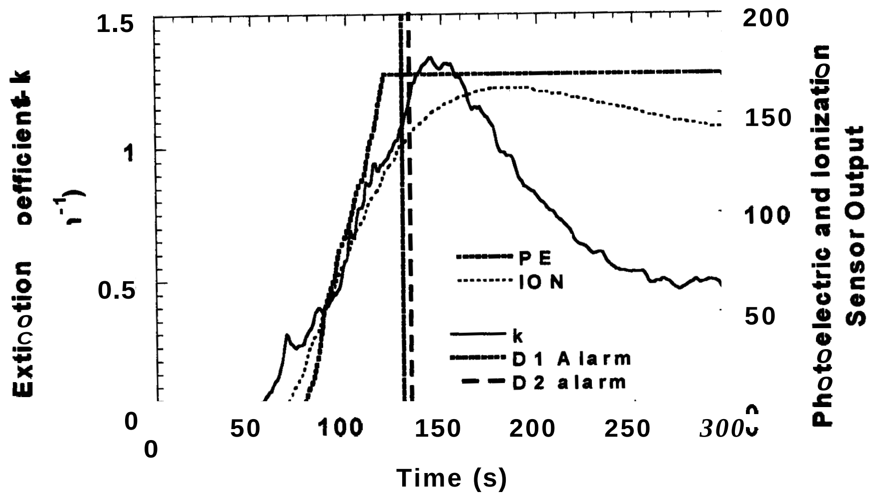

Figure 8. Smoke level for test fire 3, smoldering cotton wicks.

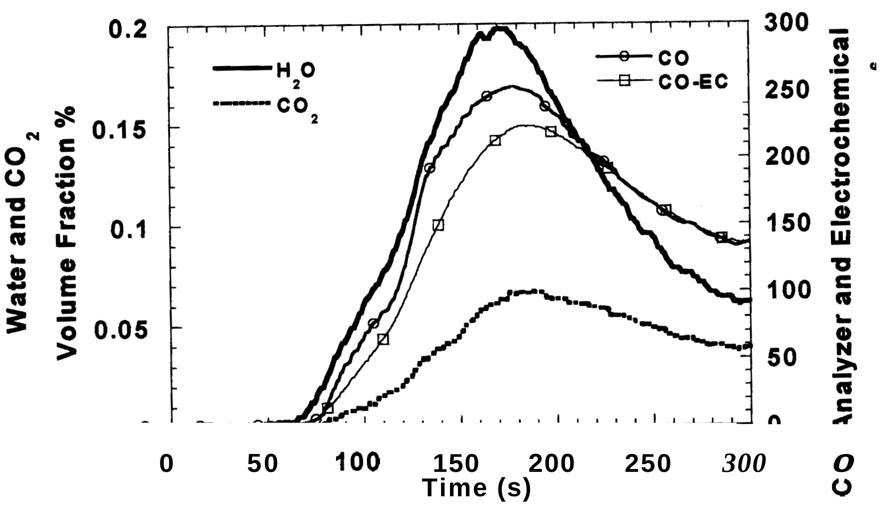

Figure 9. Gas signatures for test fire 3, smoldering cotton wicks.

vertical riser. The fan speed was set to 10 Hz yielding a mean flow velocity of 0.25 m/s at the test section. At time = 0, **40** volts AC power was applied to the nichrome wire which was sufficient to start the plastics to pyrolyze and emit smoke and gases. The power was removed at 80 s and the pyrolyzing eventually stopped. Figures 10 and 11 show representative smoke and combustion gas production for this source. The photoelectric, ionization signal, and extinction coefficient all began to rise at 30 s. The photoelectric signal reached its maximum output at 50 s while the extinction coefficient and ionization signal continued to rise peaking at 90 s and 105 s respectively. The spot-type aircraft detector alarmed at 66 s, while the draw-through detector alarmed at 88 s. The combustion gas production levels were low compared to the other smolder sources.

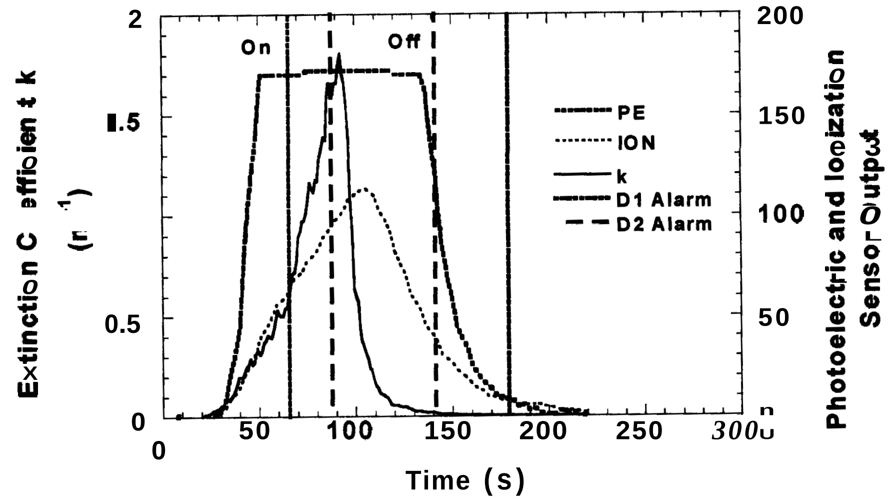

Figure 10. Smoke level for test fire 4, pyrolyzing plastics.

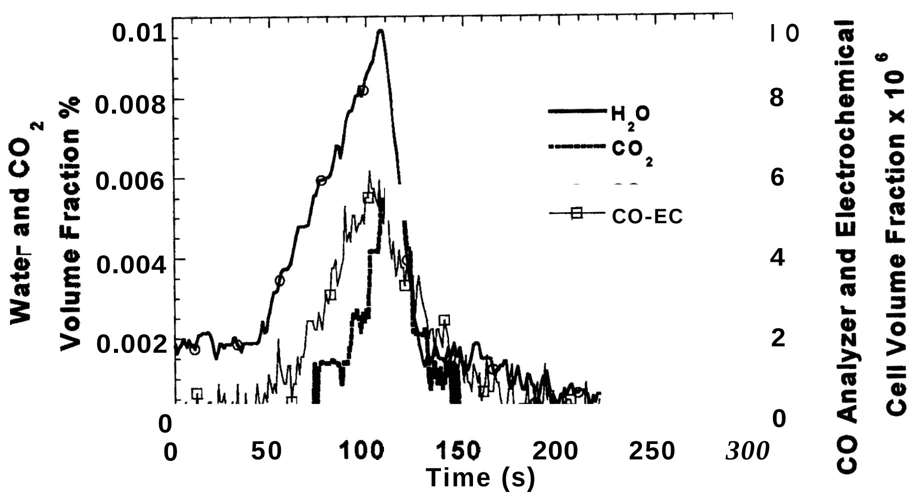

Figure 11. Gas signatures for test fire 4, pyrolyzing plastics.

The CO volume fraction peaked at 6 x 10^{-6}, while the CO_2 volume fraction peaked at $5.0x10^{-3}$ % above the background level. No rise in the water concentration was observed. Air temperature rise was about 1 °C above ambient temperature.

The dust aerosol was generated by injecting ISO 12103-1 fine grade Arizona test dust at a constant rate from a powder screw feeder. With the fan speed set at 10 Hz, the dust was fed into the duct at time = 0. Figure 12 shows the extinction coefficient and detector output for this source. The extinction coefficient started to rise at about 12 s followed by the photoelectric and ionization signals 10 s later. The extinction was above 2 m^{-1} at 30 s and stayed between 2 m^{-1} and 2.5 m^{-1} until the dust flow was stopped at

100s and the remaining dust blown out of the duct. The photoelectric signal reached its maximum output at about 25 s, while the ionization continued to rise until the dust flow was stopped. The spot-type aircraft detector alarmed at 59 s, while the draw-through detector alarmed at 100 s.

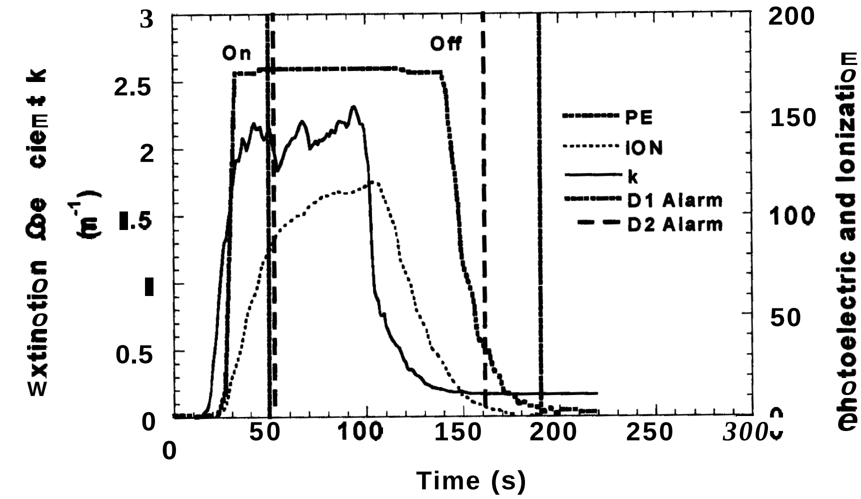

Figure 12. Particulate level for nuisance source 1, dust exposure.

The oil mist aerosol was generated by nebulizing cooking oil from a bank of 10 medical inhalent nebulizers located at the bottom of the vertical riser of the FE/DE. This aerosol is a surrogate for hydraulic oil or non-volatile mists introduced in a cargo compartment intentionally (cargo treatment) or unintentionally. The fan speed was set at 7 Hz yielding at mean flow velocity of 0.15 m/s at the test section, and the nebulizers were

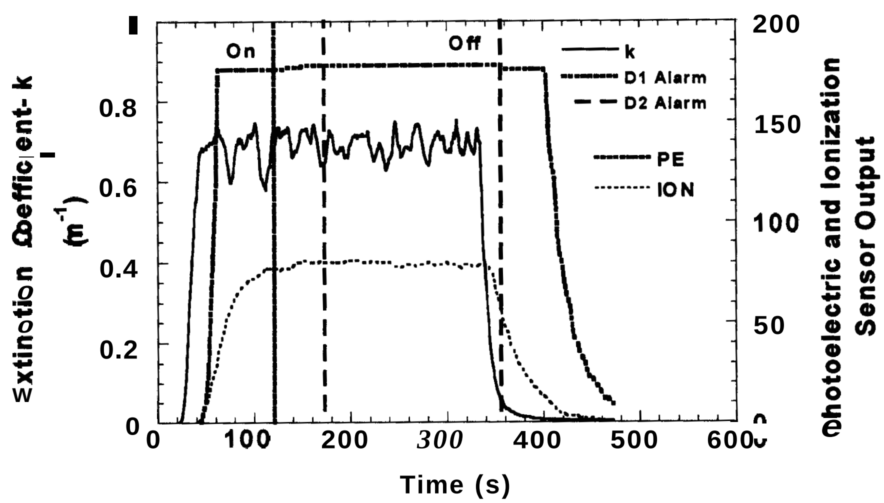

Figure 13. Particulate level for nuisance source 2, oil mist exposure.

started at time = 0. Figure 13 shows the extinction coefficient and detector outputs for this source. The extinction coefficient started to rise at 20 s and reached nearly steady values between 0.6 m^{-1} and 0.7 m^{-1} within 10 s. The photoelectric and ionization signals began to rise at 40 s with the photoelectric signal saturating at about 60 s while the ionization signal continued to rise until reaching a steady value at approximately 120 s. The spot-type aircraft detector alarmed at 120 s, while the draw-through detector alarmed at 173 s.

4. Conclusions

Six plausible fire and nuisance alarm scenarios for aircraft cargo compartments were reproduced in the FE/DE. The data gathered contains particulate, combustion gas and temperature rise values that may be used to identify sensor combinations to discriminate between fire and non-fire conditions. Background levels of particulate, combustion gas and temperature fluctuations need to be included in any analysis leading to sensor selection and alarm algorithm design.

5. References

[1] D., "Aircraft Cargo Compartment Smoke Detector Alarm Incidents on U.S.-Registered Aircraft, 1974-1999," DOT/FAA/AR-TN00/29, U.S. Dept. of Trans., Federal Aviation Administration, 2000.

[2] Grosshandler, W., (editor), "Nuisance Alarms in Aircraft Cargo Areas and Critical Telecommunications Systems: Proceedings of the 3rd MST Fire Detector Workshop," December 4-5, 1997, NISTIR 6146, National Institute of Standards and Technology, Gaithersburg, MD, March 1998.

[3] "Cargo Compartment Fire Detection Instruments," Aerospace Standard, AS 8036, Society of Automotive Engineers, Inc., Warrendale, PA, 1985.

[4] Cleary, T., and Grosshandler, W., "Survey of Fire Detection Technologies and System Evaluation/Certification Methodologies and their Suitability for Aircraft Cargo Compartments," NISTIR 6356, National Institute of Standards and Technology, Gaithersburg, MD, July 1999.

[5] Cleary, T., and Donnelly, M., "Improved Fire Detection in Aircraft Cargo Compartments," NISTIR in preparation, National Institute of Standards and Technology, Gaithersburg, MD, 2001.

[6] Cleary, T., Grosshandler, **W.,** and Chernovsky, A., "Smoke Detector Response to Nuisance Aerosols," Proceeding of the 11th International Conference on Automatic Fire Detection "AUBE '99," March 16-18, 1999, Gerhard Mercator University, Duisburg, Germany, Luck, H., Ed., pp 32-41, 1999.

[7] Cleary, T., Grosshandler, **W.,** Nyden, M., and Rinkinen, **W.,** "Signatures of Smoldering/Pyrolyzing Fires for Multi-element Detector Evaluations," Proc. of the 7th Inter. Conf. on Fire Science and Eng., Interflam '96, Cambridge, England, March 1996.